







# Polarization modulation effect of BeO on AlGaN/GaN high-electron-mobility transistors

EP

Cite as: Appl. Phys. Lett. **115**, 103502 (2019); <https://doi.org/10.1063/1.5108832>

Submitted: 02 May 2019 . Accepted: 17 August 2019 . Published Online: 06 September 2019

Weijie Wang, Seung Min Lee, Sara Pouladi, Jie Chen, Shahab Shervin, Seonno Yoon , Jung Hwan Yum, Eric S. Larsen , Christopher W. Bielawski, Bikramjit Chatterjee , Sukwon Choi , Jungwoo Oh , and Jae-Hyun Ryou 

## COLLECTIONS

EP

This paper was selected as an Editor's Pick



View Online



Export Citation



CrossMark

## Lock-in Amplifiers up to 600 MHz

starting at

\$6,210



 Zurich Instruments

Watch the Video



AIP  
Publishing

# Polarization modulation effect of BeO on AlGaIn/GaN high-electron-mobility transistors

Cite as: Appl. Phys. Lett. **115**, 103502 (2019); doi: [10.1063/1.5108832](https://doi.org/10.1063/1.5108832)

Submitted: 2 May 2019 · Accepted: 17 August 2019 ·

Published Online: 6 September 2019





View Online



Export Citation



CrossMark

Weijie Wang,<sup>1,2,a)</sup> Seung Min Lee,<sup>3,a)</sup> Sara Pouladi,<sup>2,4</sup> Jie Chen,<sup>2,4</sup> Shahab Shervin,<sup>1,2</sup> Seonno Yoon,<sup>3</sup>  Jung Hwan Yum,<sup>5</sup> Eric S. Larsen,<sup>5,6</sup>  Christopher W. Bielawski,<sup>5,6</sup> Bikramjit Chatterjee,<sup>7</sup>  Sukwon Choi,<sup>7</sup>  Jungwoo Oh,<sup>3,b)</sup>  and Jae-Hyun Ryou<sup>1,2,4,b)</sup> 

## AFFILIATIONS

<sup>1</sup>Department of Mechanical Engineering, University of Houston, Houston, Texas 77204-4006, USA

<sup>2</sup>Advanced Manufacturing Institute (AMI) and Texas Center for Superconductivity at UH (TcSUH), University of Houston, Houston, Texas 77204, USA

<sup>3</sup>School of Integrated Technology, Yonsei Institute of Convergence Technology, Yonsei University, Incheon 21983, South Korea

<sup>4</sup>Materials Science and Engineering Program, University of Houston, Houston, Texas 77204, USA

<sup>5</sup>Center for Multidimensional Carbon Materials (CMCM), Institute for Basic Science (IBS), Ulsan 44919, South Korea

<sup>6</sup>Department of Chemistry and Department of Energy Engineering, Ulsan National Institute of Science and Technology (UNIST), Ulsan 44919, South Korea

<sup>7</sup>Department of Mechanical Engineering, The Pennsylvania State University, University Park, Pennsylvania 16802, USA

<sup>a)</sup>Contributions: W. Wang and S. M. Lee contributed equally to this work.

<sup>b)</sup>Authors to whom correspondence should be addressed: [jungwoo.oh@yonsei.ac.kr](mailto:jungwoo.oh@yonsei.ac.kr) and [jryou@uh.edu](mailto:jryou@uh.edu)

## ABSTRACT

We investigate the polarization modulation effect of a single-crystalline BeO layer on AlGaIn/GaN high-electron-mobility transistors (HEMTs). The BeO layer with macroscopic polarization on top of the AlGaIn barrier layer increases the 2-dimensional electron gas density in the triangular quantum well (QW) at the interface of the AlGaIn/GaN heterostructure. Electronic band bending of BeO and a deeper triangular QW observed from the simulated conduction band profile indicate that the BeO layer can modify the polarization field at the AlGaIn/GaN interface. A ~20-nm-thick single-crystalline BeO thin film is grown on AlGaIn/GaN HEMTs by atomic-layer deposition. Room-temperature and variable-temperature Hall-effect measurements confirm that the HEMT with BeO forms a channel with a 14% increase of the sheet carrier concentration as compared with a conventional HEMT. An improved output performance is also observed in the *I*-*V* characteristics which confirms the polarization modulation effect of the BeO layer.

Published under license by AIP Publishing. <https://doi.org/10.1063/1.5108832>

Recent development in GaN-based high-electron-mobility transistor (HEMT) technology enables the realization of high-power and high-frequency devices in power and RF electronics.<sup>1</sup> The wide-bandgap Group III-nitride (III-N) semiconductors offer many advantages in HEMTs such as a high breakdown voltage, high saturation current, and excellent carrier confinement. However, the HEMTs still suffer from various negative effects such as current collapse, gate leakage, junction heating, and trap effect for high voltage operation.<sup>2,3</sup> Moreover, conventional  $\text{Al}_x\text{Ga}_{1-x}\text{N}/\text{GaN}$  HEMTs with typically  $x \leq 25\%$  show limited sheet concentrations in the channel consisting of 2-dimensional electron gas (2DEG), e.g.,  $\leq 1 \times 10^{13} \text{ cm}^{-2}$ . Increasing the AlN mole fraction ( $x$ ) can further enhance the 2DEG density; however, it will also introduce additional technical challenges, such as an

increasing lattice mismatch between AlGaIn and GaN. The authors previously demonstrated a significant increase in 2DEG by external bending of the heterostructure, which enhances the piezoelectric polarization.<sup>4,5</sup> However, the enhancement can only be realized in mechanically bendable thin-film structures which require a layer-transfer process followed by the removal of a brittle substrate.<sup>6,7</sup>

BeO (nonsingle-crystalline) thin films grown by atomic layer deposition (ALD) were explored and demonstrated as a gate dielectric material for Si and III-V metal/oxide/semiconductor field-effect transistors (MOS-FETs) to utilize their excellent properties such as a large binding energy and an ultrawide-bandgap energy.<sup>8</sup> Recently, the authors demonstrated single-crystalline  $\alpha$ -BeO (wurtzite structure) thin films on GaN by epitaxial growth using ALD.<sup>9</sup> The single-crystalline

BeO shows a low interface-trap density and superior thermal conductivity ( $\kappa_c = 370$  W/m K at 300 K) and stability,<sup>9,10</sup> which makes the BeO a promising material for the isolation and passivation of III-N HEMTs with efficient heat dissipation. Furthermore, single-crystalline wurtzite BeO can offer additional functionality in AlGaIn/GaN HEMTs. A (0001) BeO film can be grown on (0001) III-N substrates, which means the out-of-plane direction of the BeO film is aligned in the [0001] crystallographic direction. In such a direction, the BeO film shows strong spontaneous and piezoelectric polarizations arising from its noncentrosymmetric crystal structure. The formation of a 2DEG channel in AlGaIn/GaN HEMTs originates from the charge at the heterointerface induced by the polarizations.<sup>11,12</sup> Therefore, the polarization field in the BeO film will modify the polarizations in the HEMTs when integrated with AlGaIn/GaN heterostructures. In the present study, we show that a single-crystalline BeO film grown on an AlGaIn/GaN HEMT can modify the total polarization fields, resulting in an increase in the 2DEG sheet density at the AlGaIn/GaN interface via both numerical simulation and experimental characterization studies of the structures and devices.

We prepared two HEMT structures in this study: a reference HEMT and a HEMT with BeO. The reference HEMT device has a typical layer structure consisting of an  $\text{Al}_{0.25}\text{Ga}_{0.75}\text{N}$  Schottky barrier layer (20 nm) and a GaN layer that are grown on a Si (111) substrate with AlN and AlGaIn buffer layers by metalorganic chemical vapor deposition. For the HEMTs with BeO (to be referred to as a BeO HEMT in this paper), a BeO layer (20 nm or 5 nm) was deposited on top of the reference HEMT heterostructure by ALD. The process conditions for ALD were described in an earlier report.<sup>13</sup> The computational simulation was carried out using a commercial 1D technology computer-aided design device simulator (STR, FETIS) for the calculation of the electronic band diagram and the carrier distribution for both the reference HEMT and BeO HEMT structures. Quantum-mechanical treatment of the carrier confinement in the HEMT structure is based on a self-consistent solution of the Poisson and Schrödinger equations. The 2DEG properties were characterized by a temperature-variable Hall-effect measurement system (Ecopia, HMS-5000). For the measurement, the BeO HEMT sample was first etched in hydrofluoric acid (HF) with a Cr mask to create an opening for the ohmic contact on the AlGaIn surface. Ti/Al/Ni/Au (20/80/50/50 nm) metal stacks were then deposited by electron-beam evaporation followed by rapid thermal annealing (RTA) at 850 °C in a nitrogen ambient for both HEMT structures. The HEMT structures were fabricated into devices with a Ti/Al/Ni/Au source and drain electrodes and an Ni/Au gate electrode.

Figure 1 schematically shows the spontaneous ( $P_{sp}$ ) and piezoelectric ( $P_{pz}$ ) polarizations in an AlGaIn/GaN HEMT epitaxial structure (Group-III polar) with a single-crystalline BeO layer. The  $P_{sp}$  of BeO ( $-0.045$  C/m<sup>2</sup>) is not significantly different from that of  $\text{Al}_{0.25}\text{Ga}_{0.75}\text{N}$  ( $\sim -0.042$  C/m<sup>2</sup>);<sup>14</sup> hence, differential spontaneous polarizations  $\Delta P_{sp}$  at the BeO/AlGaIn interface are negligible. Piezoelectric constants and stiffness constants of BeO are  $e_{13} = -0.02$  C/m<sup>2</sup>,  $e_{33} = 0.02$  C/m<sup>2</sup>,  $c_{13} = 4.70 \times 10^{12}$  dynes/cm<sup>2</sup>, and  $c_{33} = 1.67 \times 10^{12}$  dynes/cm<sup>2</sup>, respectively.<sup>14</sup> The piezoelectric constants of BeO are smaller than those of GaN and AlN. However, when a large in-plane tensile strain is induced in the BeO layer, a substantial piezoelectric polarization field  $P_{pz}$  forms in the BeO, which changes the electronic band diagram of the heterostructure. This results in the modification of the energy levels that create the triangular quantum well (QW) at the AlGaIn/GaN interface where the 2DEG channel is formed.

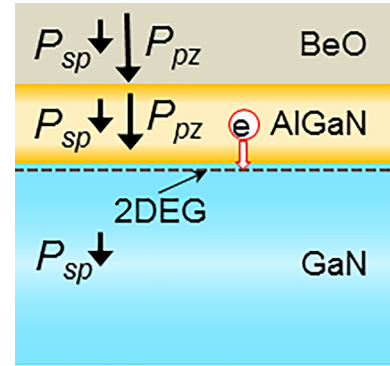


FIG. 1. Schematic representation of polarization fields for the HEMT structure with single-crystalline BeO.

Simulated electronic band diagrams of the reference HEMT and BeO HEMT are compared. The previous reports on the electronic properties of BeO are limited and the electronic band structure of BeO still remains uncertain. The authors estimated the band structure of the BeO and BeO/(Al)GaIn interface from the ALD-grown BeO film. A bandgap energy of 8.3 eV, a valence band maximum (VBM) of 4.96 eV, and an electron affinity (EA) of 0.36 eV were measured for the BeO film by reflection electron energy loss spectroscopy (REELS) and ultraviolet photoelectron spectroscopy (UPS).<sup>13</sup> The authors have reported that the epitaxial growth of BeO on GaN is possible even with a significant lattice mismatch [e.g.,  $\sim 18\%$  using a formula  $(a_s - a_l)/a_l$  for a BeO film ( $a_l = 2.698$  Å) on a GaN substrate ( $a_s = 3.186$  Å)], via domain-matching epitaxy (DME) to reduce the lattice-mismatching strain.<sup>15</sup> A relaxation degree of 20.8% was calculated from the DME-BeO by a reciprocal space map measured by high-resolution x-ray diffraction. An equivalent lattice constant of BeO is then calculated as 2.9 Å which is to be applied in the simulation. After the parameters for BeO were defined, the simulation for both structures was performed. Figure 2 shows the simulated conduction band minimum profiles. For the reference HEMT shown in a red dot-dashed line, the negative spontaneous and piezoelectric polarization fields cause the band bending of AlGaIn. As a result, a triangular QW is formed below the Fermi level (blue dashed line). The 2DEG is induced due to the negative total polarization fields and the charge density ( $\rho$ ) in the QW being related to the total polarization by the equation

$$-\rho = \nabla \cdot (P_{pz} + P_{sp}), \quad (1)$$

where  $P_{pz}$  is the piezoelectric polarization and  $P_{sp}$  is the spontaneous polarization. The 2DEG sheet density for the reference HEMT is calculated as  $9.2 \times 10^{12}$  cm<sup>-2</sup>. For the BeO HEMT shown in a green solid line, the induced  $P_{pz}$  of BeO is in a negative direction due to the tensile in-plane strain in the BeO layer. Since the  $P_{sp}$  of BeO is also in the negative direction,<sup>16–18</sup> the total polarization fields of this three-layered structure are increased, which results in a higher 2DEG charge density. The electronic band bending of both BeO and AlGaIn layers due to the negative polarization fields is observed and the triangular QW at the AlGaIn/GaN interface is deeper below the Fermi level than that of the reference HEMT as shown by the dashed green and red arrows which indicate the location of QW bottoms of the BeO HEMT and reference HEMT, respectively. The 2DEG sheet density for BeO HEMT is

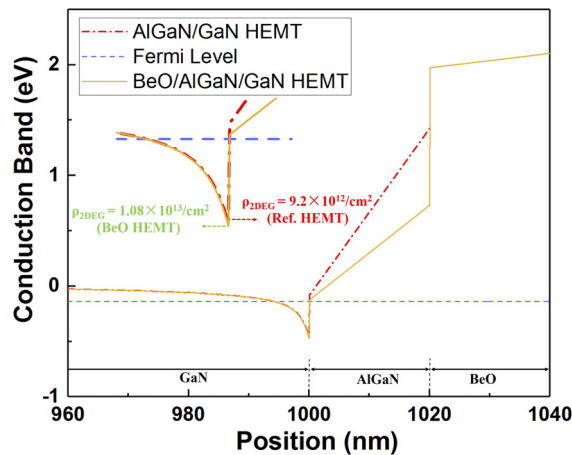


FIG. 2. Simulated conduction band minimum profile of the BeO HEMT (green solid line) and the reference HEMT (red dot-dashed line).

calculated to be  $1.08 \times 10^{13}/\text{cm}^2$ . Based on the simulation results, a 17% increase in the 2DEG sheet concentration is estimated.

Room-temperature Hall-effect measurement results of the reference and BeO (20 nm) HEMT structures are shown in Table I. The 2DEG sheet concentration of the reference HEMT was measured to be  $9.22 \times 10^{12} \text{ cm}^{-2}$  which is very close to the simulated result of  $9.2 \times 10^{12} \text{ cm}^{-2}$ . A high electron mobility of  $1430 \text{ cm}^2/\text{Vs}$  was also observed. For the BeO HEMT, a 2DEG sheet density of  $1.05 \times 10^{13} \text{ cm}^{-2}$  was measured, which corresponds to an  $\sim 14\%$  increase in the electron concentration in the channel, while the mobility remains at a similar value. Hall coefficients along two diagonal directions show a good consistency due to the square shape. The coefficients at room temperature are  $-1.69 \text{ cm}^3/\text{C}$  and  $-1.69 \text{ cm}^3/\text{C}$  for the directions of the reference HEMT and  $-1.5 \text{ cm}^3/\text{C}$  and  $-1.49 \text{ cm}^3/\text{C}$  for the BeO HEMT. The conductivity value of the BeO HEMT shows an increase of 11% compared to that of the reference HEMT. Temperature-variable Hall-effect measurement was also performed and the results are shown in Fig. 3. The inset shows a schematic cross section of the Hall-effect measurement sample of a BeO HEMT. The reference HEMT and BeO HEMT show the same trend in both the electron sheet concentration and mobility when plotted vs temperature. However, the BeO HEMT demonstrates a higher level of electron sheet concentration which represents an increase of the 2DEG sheet density. The decrease in the carrier density after 250 K can be attributed to the thermal escape of carriers out of the triangular QW.<sup>19,20</sup> The BeO HEMT also shows a smaller decrease in the carrier density than the reference HEMT at a higher temperature, which suggests a deeper QW of the BeO HEMT. The 2DEG mobility values for both HEMT structures are also shown in the secondary y-axis of Fig. 3. A small difference of 2% is found between the HEMTs. The

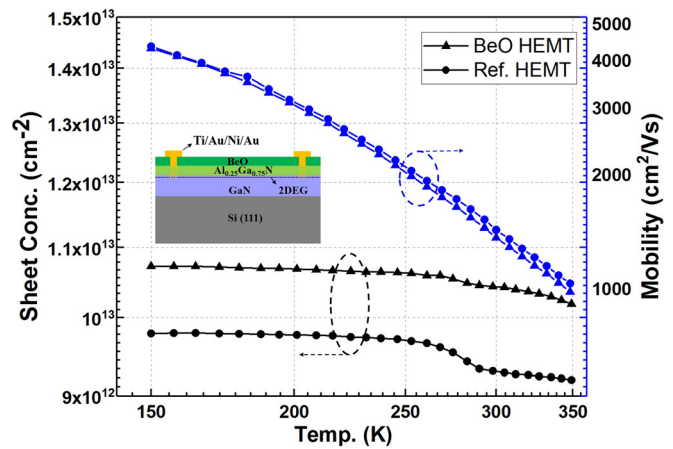


FIG. 3. Sheet concentration (primary y-axis) and mobility of carriers (secondary y-axis) from variable-temperature Hall-effect measurements of the BeO HEMT and the reference HEMT. The inset shows the schematic cross section of the BeO HEMT structure for van-der-Pauw Hall measurement.

electron mobility decreases with a higher temperature, i.e., from  $4300 \text{ cm}^2/\text{Vs}$  at 135 K to around  $1000 \text{ cm}^2/\text{Vs}$  at 350 K. The temperature dependence of mobility here mostly arises from the temperature dependence of scattering due to acoustic phonons.<sup>21</sup> Both room-temperature and variable-temperature Hall-effect measurements show a significant increase of the 2DEG sheet concentration for the BeO HEMT and the increased value (14%) is also close to the simulated result (17%).

The output characteristics were measured for both HEMT devices with gate length  $L_g = 6 \mu\text{m}$ , gate-drain distance  $L_{gd} = 6 \mu\text{m}$ , and gate-source distance  $L_{gs} = 3 \mu\text{m}$ . For the comparison of devices, the BeO HEMT with a 5-nm-thick BeO layer was fabricated to compare with the reference HEMT with similar threshold voltages. By decreasing the BeO thickness from 20 nm to 5 nm,  $V_{th}$  changes from  $-4.8 \text{ V}$  to  $-4.2 \text{ V}$  which is closer to  $-3.8 \text{ V}$  of the reference HEMT (data not shown here). Figure 4 shows the DC output characteristics with the  $V_{ds}$  ranging from 0 V to 10 V. The saturation drain currents of the BeO HEMT at  $V_g = -1$  to  $-3 \text{ V}$  are higher than those of the reference HEMT by 10% or more than the current change with the threshold voltage difference, which reflects a higher 2DEG density in the BeO HEMT. In addition, the off-state drain current, which is mostly caused by the gate leakage current below the threshold voltage, of the BeO HEMT ( $\sim 6 \times 10^{-4} \text{ mA/mm}$  at  $V_g = -10 \text{ V}$ ) is 3 orders of magnitude lower than that of the reference HEMT ( $\sim 5 \times 10^{-1} \text{ mA/mm}$ ) (data not shown here). However, the saturation current of the BeO HEMT at  $V_g = 0 \text{ V}$  is slightly higher than that of the reference HEMT. Furthermore, both HEMTs show a slight current collapse behavior at  $V_g = 0 \text{ V}$ , which requires further investigation whether self-heating takes place, overshadowing the effect of the 2DEG density difference.

TABLE I. Room temperature Hall-effect measurement results of the reference AlGaN/GaN HEMT and the HEMT with BeO.

	Sheet conc. ( $\text{cm}^{-2}$ )	Mobility ( $\text{cm}^2/\text{Vs}$ )	Conductivity ( $\Omega^{-1} \text{ cm}^{-1}$ )	Average Hall coef. ( $\text{cm}^3/\text{C}$ )
Ref. HEMT	$-9.22 \times 10^{12}$	1430	844	-1.69
HEMT w/BeO	$-1.05 \times 10^{13}$	1400	938	-1.50



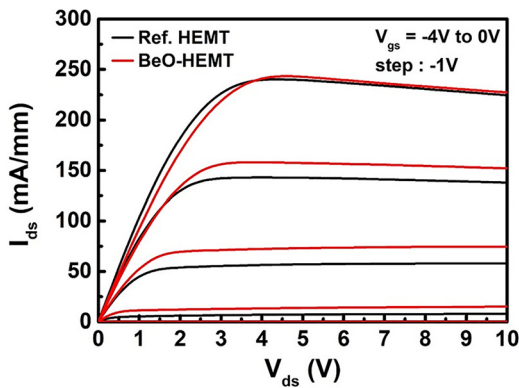


FIG. 4. Output characteristics of the 5-nm BeO HEMT (red) and the reference HEMT (black).

Interface trap density and total polarization charge change can both modify the 2DEG density. The basic expression for sheet charge concentration in the HEMT device is given by<sup>22</sup>

$$n_s = \sigma_{pol} - \frac{\epsilon_{AlGaIn}}{q \cdot d_{AlGaIn}} [\phi_{Bn} + E_F(n_s) - \Delta E_C], \quad (2)$$

where  $\sigma_{pol}$  is the total spontaneous and piezoelectric polarization induced charge concentration,  $\epsilon_{AlGaIn}$  and  $d_{AlGaIn}$  are the permittivity and thickness of AlGaIn,  $q$  is the charge of the electron,  $E_F(n_s)$  is the difference between the Fermi level and the bottom of the conduction band in the GaN layer,  $\phi_{Bn}$  is the Schottky barrier height, and  $\Delta E_C$  is the conduction band offset at the AlGaIn/GaN interface. When a single crystalline BeO layer is deposited on AlGaIn by ALD, it can reduce the interface trap density resulting from the efficient passivation of the GaN dangling bonds with crystalline BeO and increase the Schottky barrier height  $\phi_{Bn}$ .<sup>23</sup> Based on Eq. (2), the reduced interface trap density and increased Schottky barrier height  $\phi_{Bn}$  will lead to a decrement of the 2DEG density. However, the measured results show the opposite which confirms that the increased 2DEG is actually generated from the increased polarization charge change of  $\sigma_{pol}$ .

In addition, the high  $\kappa_c$  of BeO offers a potential thermal benefit by enhancing the heat dissipation away from the device active region. A coupled electrothermal simulation was performed to demonstrate the effectiveness of BeO films as heat spreaders for an AlGaIn/GaN HEMT operating under 5 W/mm. As shown in Fig. 5, a 2- $\mu$ m-thick BeO film can reduce the device peak temperature by 16% as compared to a device employing a standard  $\text{Si}_3\text{N}_4$  passivation layer.

In summary, we have studied the effect of the BeO layer on a conventional HEMT via both numerical simulation and experimental demonstration. The simulated conduction band of the BeO HEMT showed a deeper triangular QW and a higher polarization induced charge density than that of the conventional HEMT. BeO HEMT was fabricated by growing an  $\sim 20$ -nm or 5-nm BeO layer on top of the AlGaIn barrier layer by ALD. Both room-temperature and variable-temperature van der Pauw Hall-effect measurements demonstrated a higher sheet carrier concentration of about 14%. The output characteristics showed an improved performance of the BeO HEMT which confirms a higher 2DEG density. The origin of 2DEG increase was discussed and we believe the surface passivation effect of BeO can

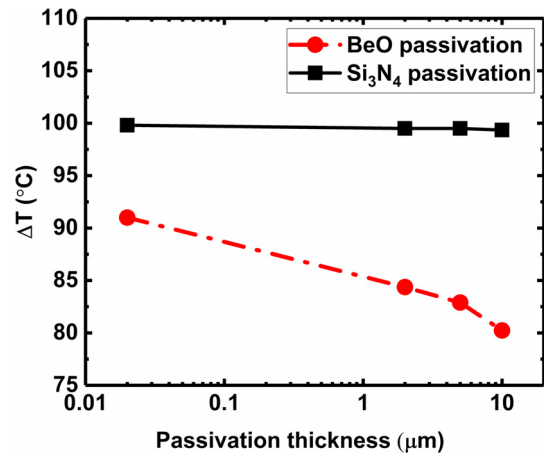


FIG. 5. Potential reduction in the HEMT peak temperature by BeO passivation in comparison to conventional  $\text{Si}_3\text{N}_{4-x}$  passivation with different thicknesses as a heat spreader.

reduce the 2DEG density while the additional polarization charge from the BeO layer can offset this effect and lead to the final increment of the 2DEG density. Besides the polarization modulation effect, other functions such as passivation and fast heat dissipation make BeO even more promising for AlGaIn/GaN HEMTs at a high voltage and high temperature operation.

This material is based upon work at the University of Houston supported by the National Science Foundation under Grant No. 1842299 [Electrical, Communications and Cyber Systems (ECCS)]. J.-H.R. also acknowledges partial support from the Texas Center for Superconductivity at the University of Houston (TcSUH) and the Advanced Manufacturing Institute (AMI). The study at Yonsei University was supported by the MIST (Ministry of Science and ICT), Korea, under the "ICT Consilience Creative Program" (IITP-2019-2017-0-01015) supervised by the IITP (Institute for Information & Communications Technology Promotion) and by the Korea Electric Power Corporation (under Grant No. R18XA06-03). Funding for efforts by the Pennsylvania State University was provided by the AFOSR Young Investigator Program (Grant No. FA9550-17-1-0141, Program Officers: Dr. Brett Pokines and Dr. Michael Kendra. This work was also monitored by Dr. Kenneth Goretti).

## REFERENCES

- <sup>1</sup>S. J. Pearton and F. Ren, *Adv. Mater.* **12**, 1571 (2000).
- <sup>2</sup>D. Nirmal, L. Arivazhagan, A. S. Augustine Fletcher, J. Ajayan, and P. Prajoun, *Superlattices Microstruct.* **113**, 810 (2018).
- <sup>3</sup>J. A. del Alamo and J. Joh, *Microelectron. Reliab.* **49**, 1200 (2009).
- <sup>4</sup>S. Shervin, S.-H. Kim, M. Asadirad, S. Ravipati, K.-H. Lee, K. Bulashevich, and J.-H. Ryou, *Appl. Phys. Lett.* **107**, 193504 (2015).
- <sup>5</sup>W. Wang, S. Shervin, S. K. Oh, J. Chen, Y. Huai, S. Pouladi, H. Kim, S.-N. Lee, and J.-H. Ryou, *IEEE Electron Device Lett.* **38**, 1086 (2017).
- <sup>6</sup>J. Chen, S. K. Oh, H. Zou, S. Shervin, W. Wang, S. Pouladi, Y. Zi, Z. L. Wang, and J.-H. Ryou, *ACS Appl. Mater. Interfaces* **10**, 12839 (2018).
- <sup>7</sup>J. Chen, S. K. Oh, N. Nabulsi, H. Johnson, W. Wang, and J.-H. Ryou, *Nano Energy* **57**, 670 (2019).

- <sup>8</sup>J. H. Yum, T. Akyol, M. Lei, T. Hudnall, G. Bersuker, M. Downer, C. W. Bielawski, J. C. Lee, and S. K. Banerjee, *J. Appl. Phys.* **109**, 064101 (2011).
- <sup>9</sup>S. M. Lee, J. H. Yum, S. Yoon, E. S. Larsen, W. C. Lee, S. K. Kim, S. Shervin, W. Wang, J.-H. Ryou, C. W. Bielawski, and J. Oh, *ACS Appl. Mater. Interfaces* **9**, 41973 (2017).
- <sup>10</sup>G. A. Slack and S. B. Austerman, *J. Appl. Phys.* **42**, 4713 (1971).
- <sup>11</sup>O. Ambacher, J. Smart, J. R. Shealy, N. G. Weimann, K. Chu, M. Murphy, W. J. Schaff, L. F. Eastman, R. Dimitrov, L. Wittmer, M. Stutzmann, W. Rieger, and J. Hilsenbeck, *J. Appl. Phys.* **85**, 3222 (1999).
- <sup>12</sup>J.-H. Ryou, P. D. Yoder, J. P. Liu, Z. Lochner, H. Kim, S. Choi, H. J. Kim, and R. D. Dupuis, *IEEE J. Sel. Top. Quantum Electron.* **15**, 1080 (2009).
- <sup>13</sup>S. M. Lee, Y. Jang, J. Jung, J. H. Yum, E. S. Larsen, S. Y. Lee, H. Seo, C. W. Bielawski, H.-D. Lee, and J. Oh, *ACS Appl. Electron. Mater.* **1**, 617 (2019).
- <sup>14</sup>T. Hanada, "Basic properties of ZnO, GaN, and related materials," in *Oxide and Nitride Semiconductors: Processing, Properties, and Applications*, edited by T. Yao and S.-K. Hong (Springer, Berlin Heidelberg, 2009), Chap. I, pp. 1–19.
- <sup>15</sup>S. M. Lee, J. H. Yum, E. S. Larsen, S. Shervin, W. Wang, J.-H. Ryou, C. W. Bielawski, W. C. Lee, S. K. Kim, and J.-W. Oh, *J. Am. Ceram. Soc.* **102**, 3745 (2019).
- <sup>16</sup>Y. Noel, C. M. Zicovich-Wilson, B. Civalieri, Ph. D'Arco, and R. Dovesi, *Phys. Rev. B* **65**, 014111 (2001).
- <sup>17</sup>F. Bernardini, V. Fiorentini, and D. Vanderbilt, *Phys. Rev. B* **56**, R10024 (1997).
- <sup>18</sup>A. Dal Corso, M. Postenak, R. Resta, and A. Baldereschi, *Phys. Rev. B* **50**, 10715 (1994).
- <sup>19</sup>T.-S. Ko, D.-Y. Lin, C.-F. Lin, C.-W. Chang, J.-C. Zhang, and S.-J. Tu, *J. Cryst. Growth* **464**, 175 (2017).
- <sup>20</sup>C. E. Dryer, A. Janotti, and C. G. Van de Walle, *Appl. Phys. Lett.* **102**, 142105 (2013).
- <sup>21</sup>A. Asgari, S. Babanejad, and L. Faraone, *J. Appl. Phys.* **110**, 113713 (2011).
- <sup>22</sup>R. Swain, K. Jena, and T. R. Lenka, *Pramana - J. Phys.* **88**, 3 (2017).
- <sup>23</sup>M. Garg, T. R. Naik, R. Pathak, V. R. Rao, C.-H. Liao, K.-H. Li, H. Sun, X. Li, and R. Singh, *J. Appl. Phys.* **124**, 195702 (2018).